Growth of ternary $PbTiO_x$ films in a combination of binary oxide atomic layer depositions

Takayuki Watanabe, Susanne Hoffmann-Eifert, Shaobo Mi, Chunlin Jia, Rainer Waser, and Cheol Seong Hwang

Citation: Journal of Applied Physics **101**, 014114 (2007);
View online: https://doi.org/10.1063/1.2422777
View Table of Contents: http://aip.scitation.org/toc/jap/101/1
Published by the American Institute of Physics

Growth of ternary $PbTiO_x$ films in a combination of binary oxide atomic layer depositions

Takayuki Watanabe,[a] Susanne Hoffmann-Eifert, Shaobo Mi, Chunlin Jia, and Rainer Waser
Institute of Solid State Research, Research Centre Jülich, 52428 Jülich, Germany and Center of Nanoelectronic Systems for Information Technology (CNI), Research Centre Jülich, 52428 Jülich, Germany

Cheol Seong Hwang[b]
School of Materials Science and Engineering, Seoul National University, Seoul 151-742, Korea

(Received 14 September 2006; accepted 29 October 2006; published online 12 January 2007)

Ternary $PbTiO_x$ films were deposited at 240 °C on Pt-covered Si substrates using a combination of liquid injection atomic layer depositions of binary TiO_x and PbO films. $Ti(OC_3H_7)_2(C_{11}H_{19}O_2)_2$ $[Ti(O\mathit{i}-Pr)_2(DPM)_2]$ and $Pb(C_{11}H_{19}O_2)_2$ $[Pb(DPM)_2]$ dissolved in ethylcyclohexane and H_2O were used as source materials. The deposition rates of Pb and Ti were enhanced in the ternary process compared to their binary processes under comparable deposition conditions. The Pb/Ti ratio of $PbTiO_x$ films saturated with an increase in Ti precursor input, while it continued to increase with an increasing Pb precursor input. The self-regulated growth nature of the Pb–O layer in the binary film growth was lost in the mixed $PbTiO_x$ process as a result of interaction with the predeposited Ti–O layer. It was confirmed that for the $PbTiO_x$ film to grow on Pt substrates, an initial incubation period is required. Both Pb–O and Ti–O layers shared a common incubation period of up to ten sequences. The incubation period was shortened by increasing the input of Pb precursor. It was independent of the input of the Ti precursor and the order of precursor supply. This variable incubation period was considered as a potential key issue for growing stoichiometric and uniform multicomponent films over three-dimensional (3D) structures. The order of precursor supply affected the effective deposition rate after the incubation period. A sequence starting with a Ti precursor injection showed a higher growth rate than a sequence that started with a Pb precursor supply. A $PbTiO_x$ film was deposited on a 3D substrate precoated with an Ir layer to demonstrate the uniformity in film thickness and cation composition. Although the present $PbTiO_x$ process does not have an ideal wide-process window in the cation composition, the $PbTiO_x$ film showed uniform coverage and the distribution of cation composition over the hole structure was within ±10%. © *2007 American Institute of Physics*. [DOI: 10.1063/1.2422777]

I. INTRODUCTION

Metal organic chemical vapor deposition (MOCVD) has been widely used for coating large active surface areas of three-dimensional (3D) nanostructures with functional thin films. The isotropic flow of precursor molecules accounts for the good step coverage of MOCVD in contrast to most physical vapor deposition processes with a straightforward flight of elements from a point source to the substrate. In the case of 3D deposition of binary oxide films, such as HfO_2 and Ta_2O_5 for capacitor applications, the homogeneity of film thickness is central, while uniformity in cation composition becomes an additional issue for multicomponent films. Recent studies have indicated a serious problem in that multicomponent oxide films deposited over 3D structures by MOCVD exhibit nonuniformity in cation composition, although film thickness appears to be uniform over the complex structure.[1–4] In MOCVD, surface reaction limiting deposition, where the deposition rate depends only on the substrate temperature, has been a common approach to achieving a homogeneous 3D coverage. However, at a mutual deposition temperature, not every precursor necessarily decomposes under the surface-reaction limiting condition. Different precursors usually have different sticking coefficients. Furthermore, a gas phase reaction among the precursors produces by-products, so that mixing precursors complicate the process. Therefore, another approach is necessary if uniform coverage of multicomponent oxide films over complex structures is to be achieved, both in cation composition and in film thickness.

Atomic layer deposition (ALD) is a surface-reaction controlled process. A saturated film growth rate against the precursor input is characteristic of ALD (Refs. 5–7) and allows homogeneity to be achieved on complex structures. The ALD process utilizes chemisorption on a predeposited layer. In multicomponent ALD, chemisorption behavior on a different predeposited cation layer is of particular interest. An ALD process typically consists of a sequential precursor and reactant gas supply, and an appropriate inert gas purge after each step. Purging ensures that any extra precursor that does not directly contribute to the chemisorption is removed from the film's surface together with extra oxidant and pumped out of the reactor. Hence, with sufficient precursor supply and adequate inert gas purging, conformal film coverage and

[a]Electronic mail: t.watanabe@fz-juelich.de
[b]Electronic mail: cheolsh@snu.ac.kr

a high controllability of film thickness, and film composition, can be expected even for nonplanar substrates. Emerging nanoimprint technology,[8] which can readily build up nanostructures, will require the 3D coverage technique for its potential applications.

In this study, $PbTiO_x$ was initially chosen to study a multicomponent ALD process, aiming finally for ALD-Pb(Zr,Ti)O_x. $PbTiO_3$-based perovskites with large switching charges were investigated in terms of their integration into ferroelectric random access memories (FeRAMs).[9,10] Due to ongoing reductions in the feature size and switching voltage, a conformal deposition of very thin films on 3D capacitor structures was required.[1,2]

Thin films of $PbTiO_x$ were deposited in a combination of two self-limiting binary processes of ALD-TiO_x and PbO.[11,12] The deposition rates of the cations and the incubation period were investigated as a function of the input of precursors using planar substrates. Although there are several papers on ALD of multicomponent oxide thin films including $PbTiO_x$,[12–21] these studies do not systematically cover the above-mentioned parameters which are critical for uniform 3D coverage. Finally, uniformity in the cation composition of a $PbTiO_x$ film deposited on a 3D structure is demonstrated.

II. EXPERIMENT

An ALD tool equipped with a pulse injection system with four independent liquid precursors and a horizontal gas flow reactor was set up for this study. The advantages of this system and the injection condition can be seen elsewhere.[12] $PbTiO_x$ films were deposited on 1×1 in.^{2} (111)Pt/ZrO_x/SiO_x/(100)Si planar substrates and 3D-structured Si substrates precovered with an Ir layer. The selected precursors were $Ti(Oi-Pr)_2(DPM)_2$ [$Ti(OC_3H_7)_2(C_{11}H_{19}O_2)_2$, diisopropoxide dipivaloylmethanato titanium] and $Pb(DPM)_2$ [$Pb(C_{11}H_{19}O_2)_2$, dipivaloylmethanato lead] dissolved in ethylcyclohexane (C_8H_{16}, ECH) with a concentration of 0.1*M* (SAES Getters S.p.A., Italy). In a multicomponent ALD process, all precursors must have the so-called ALD window[5] at a common deposition temperature because the substrate temperature cannot be changed during the process. Thus, the deposition temperature was set to 240 °C. This temperature is below the thermal decomposition temperatures of the present precursors.[11,12] H_2O gas was supplied as an oxidant by its own vapor pressure for 1 s from a reservoir kept at 10 °C. Following the precursor injection and the H_2O gas supply, the reactor was purged for 5–20 s with 200 SCCM (cubic centimeter per minute at STP) Ar gas for all investigations. The reactor pressure was kept at 1 Torr. We refer to a deposition unit of one Ti–O or one Pb–O layer as one cycle, and to a combination of the cycles for the growth of a $PbTiO_x$ film as one sequence. The unit cycle is repeated in a sequence to adjust the film composition.

The deposition rates of the constituent elements and the film composition, as well as the film thickness, were calculated using wavelength dispersive x-ray fluorescence (XRF) spectroscopy. A cross section and local cation composition of a $PbTiO_x$ film deposited on a 3D substrate were analyzed by transmission electron microscopy (TEM) combined with energy dispersive x-ray (EDX) spectroscopy. The structural properties, morphology, and residual C content in the films were analyzed by x-ray diffraction (XRD), atomic force microscopy (AFM), and x-ray photoelectron spectroscopy (XPS), respectively.

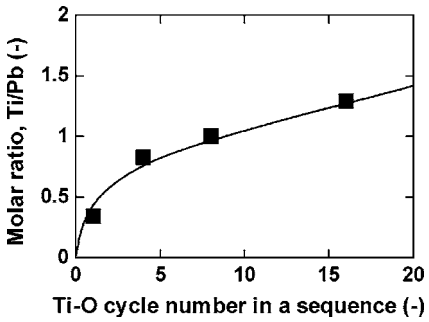

FIG. 1. Molar ratio of Ti to Pb in the $PbTiO_x$ films as a function of the repetition number of Ti–O cycle against one Pb–O cycle. The injected precursor volumes were 27 and 45 μl/cycle for $Pb(DPM)_2$ and $Ti(Oi\text{-}Pr)_2(DPM)_2$, respectively.

III. RESULTS AND DISCUSSION

A. Self-regulated growth behavior in ALD-$PbTiO_x$ processes

Two self-regulated processes of ALD-PbO and TiO_x were mixed to deposit $PbTiO_x$ films. In the multicomponent ALD process, the input of precursors was initially set at a volume that was high enough to achieve saturated deposition rates in their binary processes. Even though the deposition temperature was very low, the process began with the Ti–O cycle in order to avoid the generation of $PbPt_x$ alloy.[22,23] In one sequence, the Ti–O cycle was repeated several times against one Pb–O cycle to adjust the film composition. This was necessary because the ALD-PbO process had a deposition rate of 4.2×10^{-10} mol/cm^2 cycle, which was approximately ten times higher than the ALD-TiO_x process (4.5×10^{-11} mol/cm^2 cycle) at deposition temperatures of 240 and 260 °C, respectively.[11,12]

Figure 1 shows the molar ratio of the cations in the deposited films as a function of the repetition number of Ti–O cycles in one sequence. In spite of the large difference in the deposition rates of ALD-PbO and TiO_x, the Ti/Pb ratio increased rapidly and approached about 1 at a cycle ratio of Ti/Pb=4. The Ti/Pb ratio in the films moderately increased with a further increase in the cycle ratio. This nonlinear change in the Ti/Pb molar ratio against the increasing repetition number of the Ti–O cycles suggests that the deposition rate of Ti was not constant throughout the repetitions, but was faster on the Pb–O layer than on the Ti–O layer. If the deposition rates of Ti and Pb in this $PbTiO_x$ process were identical to those in their binary processes, ten repetitions of the Ti–O cycles would have been necessary for one Pb–O cycle to achieve a molar ratio of 1. There are two possible explanations for this behavior: one is that the Pb–O layer has a higher bonding site density for the Ti precursor molecule

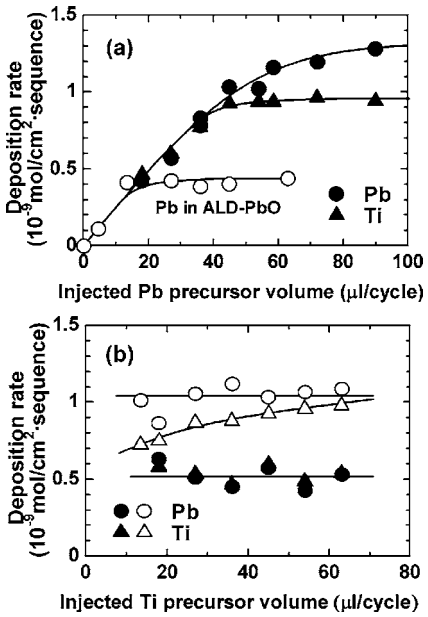

FIG. 2. Deposition rates of Pb and Ti at varied volumes of Pb and Ti precursor injections. Unit sequence of $8\times(\mathrm{Ti-O})\text{-}1\times(\mathrm{Pb-O})$ was repeated 25 times. (a) Fixed volume of Ti precursor injection at 45 μl/cycle. (b) Fixed volume of Pb precursor injection at 27 μl/cycle (closed symbol) and 45 μl/cycle (opened symbol), respectively. The open circles show the deposition rate of Pb in an ALD-PbO process at 240 °C (Ref. 11).

than the Ti–O layer itself, and the other is that the chemisorption of the Ti precursor onto the Pb–O layer is more active than chemisorption on the Ti–O layer.

The self-regulated growth rate and incorporation behavior of Pb and Ti in the $PbTiO_x$ films were investigated by changing the input of precursors per cycle. Based on the result shown in Fig. 1, the Ti–O cycle number in one sequence was set to 8 for one Pb–O cycle for this experiment. The unit sequence described as $8\times(\mathrm{Ti-O})\text{-}1\times(\mathrm{Pb-O})$ was repeated 25 times. This repetition number gives approximately a 10 nm thick amorphous $PbTiO_x$ film.

Figures 2(a) and 2(b) show the variations in the deposition rates of Pb and Ti as a function of the injected precursor volume in a unit of mol/cm^2 sequence. To investigate the self-regulated growth behavior, the precursor input in one sequence, either V(Pb) or V(Ti), was varied while the input of the other precursor was kept constant. V(Ti) was fixed at 45 μl/cycle in order to test what effect V(Pb) has. Then V(Pb) was fixed at 27 and 45 μl/cycle when the effects of V(Ti) were being studied. For comparison, the deposition rate of Pb in the binary ALD-PbO process is also shown in Fig. 2(a).[11] The incorporation of Pb and Ti into the $PbTiO_x$ films was quite different than in their respective binary oxide processes. We will discuss the deposition rate of Ti first. Figure 2(a) shows that the deposition rate of Ti increased with increasing V(Pb) up to a volume of ~40 μl/cycle, although V(Ti) was fixed at a given value (45 μl/cycle). When V(Pb) increased above ~40 μl/cycle, the Ti deposition rate saturated at $\sim1\times10^{-9}$ mol/cm^2 sequence. The average deposition rate of Ti per Ti–O cycle was calculated to be 1.3×10^{-10} mol/cm^2 cycle. This value is three times higher than the deposition rate in the ALD-TiO_x process, 4.5×10^{-11} mol/cm^2 cycle, which was performed under similar experimental conditions.[12] This deposition behavior of Ti suggests that the incorporation of Ti into the $PbTiO_x$ films by chemisorption of the Ti precursor on the predeposited Pb–O layer was highly enhanced compared to that on the Ti–O surface. Although it remains unclear whether this enhancement is due to higher-density bonding sites or to a higher chemical activity of the Ti precursor on the Pb–O layer, the saturation behavior shown in Fig. 2(a) implies that the Pb–O surface allows high-density bonding with the Ti precursor. It appears that Ti precursor molecules chemisorb on the Pb–O surface as long as the sites are available. This is further confirmed by the results shown in Fig. 2(b).

When V(Pb) was fixed at 27 μl/cycle, the deposition rate of Ti decreased to $\sim5\times10^{-10}$ mol/cm^2 sequence irrespective of V(Ti) in the tested V(Ti) range. The bonding sites for the Ti precursor on the Pb–O layer were probably insufficient to catch the given Ti precursor, which meant that the deposition rate of Ti was kept accordingly low. When V(Pb) was increased to 45 μl/cycle, the deposition rate of Ti also increased. However, under this V(Pb) condition, even V(Ti) of up to 63 μl/cycle proved insufficient for occupying all of the bonding sites provided by the Pb–O layer. Therefore, the Ti deposition rate continued to increase with increasing V(Ti) under these growth conditions.

We will now turn the discussion to focus on the incorporation behavior of Pb in the $PbTiO_x$ films. Figure 2(a) shows that the deposition rate of Pb is certainly higher in the $PbTiO_x$ layer than that in the binary PbO process. This suggests that the Ti–O surface enhanced the chemisorption of Pb precursor molecules in comparison to the Pb–O surface, in a similar manner to the Pb–O surface for the Ti precursor. Up to V(Pb) of ~40 μl/cycle, most of the injected Pb precursor molecules chemisorbed on the Ti–O (or Pb–Ti–O) surface when V(Ti) was 45 μl/cycle for as long as the bonding sites for the Pb precursor molecules were available [Fig. 2(a)]. Therefore, the self-regulated Pb/Ti ratio of 1 was obtained for the $PbTiO_x$ film under these deposition conditions [see Fig. 3(a)]. It should be noted that the Ti deposition rate is also determined by the bonding sites provided on the Pb–O surface, so that the emergence of the self-regulated composition of Pb/Ti ~ 1 in this range is quite natural. However, the incorporation of Pb into the $PbTiO_x$ films under the condition of V(Pb) > ~40 μl/cycle is rather different from that of V(Pb) < ~40 μl/cycle. Figure 2(a) shows that the deposition rate of Pb kept increasing with increasing V(Pb) despite the saturation of the deposition rate of Ti for V(Pb) > ~40 μl/cycle. If Pb deposition was simply determined by the availability of bonding sites on the Ti–O surface, the deposition rate of Pb would have been saturated when the Ti deposition rate was saturated. It appears that there is another factor that further enhances the incorporation of Pb into the $PbTiO_x$ film when all available bonding sites on the Ti–O surface were consumed by the Pb precursor molecules. This could be due to the catalytic activity of the Ti–O surface, which decomposes the metal organic precursor molecules. A mole area density of 1.0×10^{-9} mol/cm^2 was calculated for a (100) plane of an ideal $PbTiO_3$ single crystal, whose lattice parameter is typically ~0.4 nm. Although the deposited films are amorphous as will be described later, a deposition

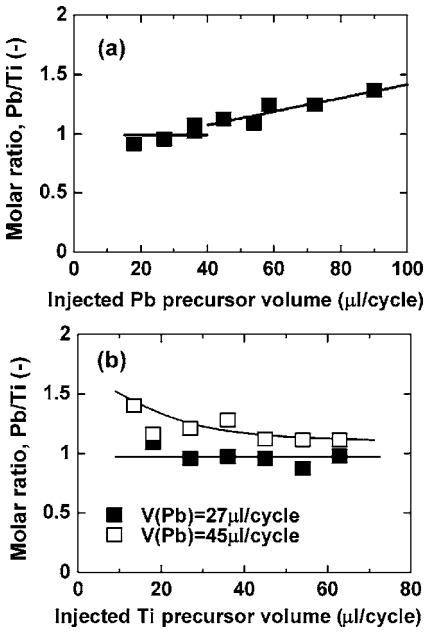

FIG. 3. Pb/Ti ratio in the $PbTiO_x$ films as a function of input of the Pb and Ti precursors. (a) Fixed volume of Ti precursor injection at 45 μl/cycle. (b) Fixed volume of Pb precursor injection at 27 μl/cycle (closed symbol) and 45 μl/cycle (open symbol), respectively.

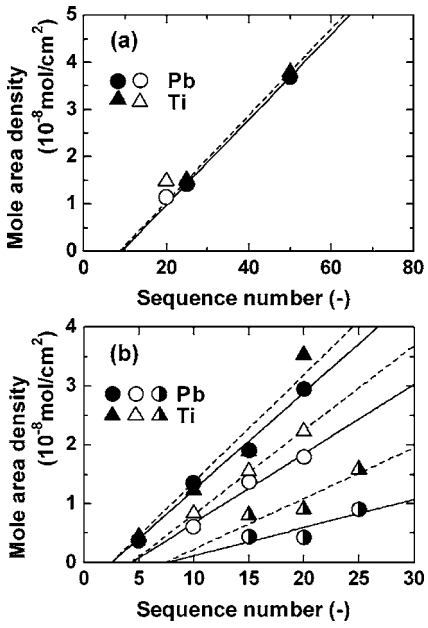

FIG. 4. Sequence number dependence of mole area densities of Pb and Ti in $PbTiO_x$ films. (a) Unit sequence: $8\times$(Ti−O)-$1\times$(Pb−O) (closed symbol) and $16\times$(Ti−O)-$1\times$(Pb−O) (open symbol). Volumes of injected Pb and Ti precursors were fixed at 27 and 45 μl/cycle for the $8\times$(Ti−O)-$1\times$(Pb−O) sequence, and 32 and 39 μl/cycle for the $16\times$(Ti−O)-$1\times$(Pb−O) sequence, respectively. (b) Unit sequence: $1\times$(Pb−O)-$16\times$(Ti−O). The closed, open, and half-open symbols correspond to the injected Pb precursor volumes of 161, 96, and 32 μl/cycle, respectively. The volume of injected Ti precursor was kept at 39 μl/cycle throughout this experiment.

rate of 1.0×10^{-9} mol/cm^2 sequence is the maximum deposition rate of Pb and Ti for an ideal layer-by-layer growth of a $PbTiO_3$ crystal from the viewpoint of ion packing density. Figure 2(a) shows that the deposition rate of Pb continued to increase above the value of 1.0×10^{-9} mol/cm^2 sequence for V(Pb)$>\sim$40 μl/cycle. Therefore, it appears that this activity is not limited to the very first layer deposited on top of the Ti–O layer. This is confirmed by the constant Pb deposition rate as a function of V(Ti) when V(Pb) was 45 μl/cycle, as shown in Fig. 2(b). Although the deposition rate of Ti decreased with decreasing V(Ti), the deposition rate of Pb remained almost constant. Even with a deficient Ti concentration on the growing film surface, the high Pb deposition rate was still maintained thanks to the catalytic influence of the Ti–O surface.

Figures 3(a) and 3(b) show the variations in the Pb/Ti molar ratio in the $PbTiO_x$ films as a function of V(Pb) with fixed V(Ti) at 45 μl/cycle, and as a function of V(Ti) with fixed V(Pb) at 27 and 45 μl/cycle, respectively. The films showed a constant stoichiometric composition in the regime of self-regulated growth under the proper precursor input conditions [V(Pb)$<\sim$40 μl/cycle in Fig. 3(a) and V(Pb)=27 μl/cycle in Fig. 3(b)], which is of crucial importance in the film deposition process for FeRAM fabrication.

B. Incubation period

An incubation period, which is the time difference between when the precursor supply was initiated and when the film growth began, is often observed for ALD processes.[24–26] The deposition rates depicted in Figs. 2(a) and 2(b) were calculated by dividing the deposited mole area density by the ALD sequence number including the incubation period. The Pb/Ti ratio is not affected by the incubation period, while the deposition rate may be more correctly calculated by dividing the deposited mole area density by an "effective" sequence number for confirming self-regulated growth. Particularly when the incubation period is not negligible, it must be treated carefully. In general, the incubation period varies depending on the precursor supply rate[24] and the substrate material.[25,26]

This variable incubation period will affect the uniformity of films grown on 3D structures. If the amount of locally supplied precursor varies from point to point over a 3D structure, the incubation period will also vary depending on where it is initiated on the structure. As a result, even if the growth rate is self-regulated after the film starts growing, the film thickness and/or film composition will have a distribution over the 3D structure. Therefore, the incubation period poses a potential problem for addressing the uniform coverage of 3D structures.

Figure 4 shows the variations in the Pb and Ti mole area density in $PbTiO_x$ films as a function of the sequence number. In Fig. 4(a), the V(Pb) and V(Ti) were fixed at 27 and 45 μl/cycle, respectively. The unit sequence is described as $8\times$(Ti−O)-$1\times$(Pb-O). This is identical to the unit sequence used for the depositions displayed in Figs. 2 and 3. For this experiment, 360 μl of the Ti precursor were injected in one sequence (45 μl/cycle$\times$8 cycles/sequence). Pb and Ti shared a common x-axis intercept, indicating the growth of Pb–O and Ti–O layers started at the same sequence after an incubation period, in this case ten sequences. The effective deposition rates of Pb and Ti calculated from the slopes in Fig. 4(a) have not been influenced by the incubation period.

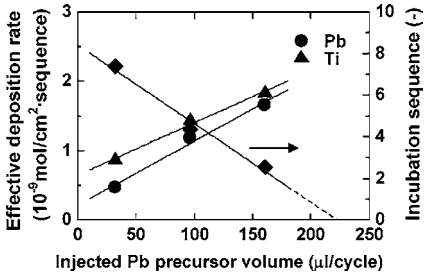

FIG. 5. Effective deposition rates of Pb and Ti, and the incubation sequence calculated from Fig. 4(b) as a function of the volume of injected Pb precursor.

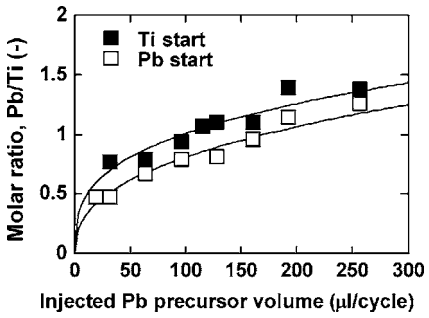

FIG. 6. Pb/Ti ratio in the $PbTiO_x$ films. Unit sequences of $16\times$(Ti–O)-1 $\times$(Pb–O) (Ti starts) and $1\times$(Pb–O)-16$\times$(Ti–O) (Pb starts) were repeated 20 times. The volume of injected Ti precursor was fixed at 39 μl/cycle.

The effective deposition rates of Pb and Ti were almost the same at 9×10^{-10} mol/cm^2 sequence. In Fig. 4(a), the open symbols indicate the mole area densities of Pb and Ti in a $PbTiO_x$ film, which was deposited by a unit sequence of $16\times$(Ti–O)-1$\times$(Pb–O). In this sequence, the Ti–O cycle number was doubled. Here V(Pb) and V(Ti) were 32 and 39 μl/cycle, respectively. Compared to the sequence of 8 $\times$(Ti–O)-1$\times$(Pb–O), the difference in V(Pb) is marginal, despite a larger amount of the Ti precursor of 624 μl being injected in this sequence. As a result, the mole area density of Pb deposited by the sequence with twice the number of Ti–O cycles was almost an extension of the line. Therefore, it is expected that increasing the input of the Ti precursor in a unit sequence does not dramatically affect the incubation period. The mole area density of Ti visibly increased in response to the doubled Ti–O cycles. This result is consistent with the result shown in Fig. 2(b), where the deposition rate of Pb was independent of V(Ti).

In Fig. 4(b), variations in the cation mole area densities in $PbTiO_x$ films deposited by a unit sequence of 1 $\times$(Pb–O)-16$\times$(Ti–O) are shown. This sequence began with the first injection of the Pb precursor. Here, three sets of precursor input, i.e., V(Pb) of 32, 96, and 161 μl/cycle with a fixed V(Ti) of 39 μl/cycle, were tested. Again, the graphs showed finite positive x-axis intercepts, suggesting that the growth of the $PbTiO_x$ film on Pt substrates requires initial incubation periods. Figure 4(b) shows that the incubation period decreases with increasing V(Pb). The variation in the incubation period given in terms of the number of deposition sequences as a function of V(Pb) is shown in Fig. 5. The linear extrapolation of the graph suggests that the incubation period will disappear when the V(Pb) is increased to $\sim$220 μl/cycle. For the present sequence with V(Pb) of 32 μl/cycle, about seven incubation sequences are required to start the growth of the $PbTiO_x$ film. This incubation period is comparable to the ten incubation sequences observed for the $8\times$(Ti–O)-1$\times$(Pb–O) or $16\times$(Ti–O)-1$\times$(Pb–O) sequences that began with the injection of the Ti precursor with comparable V(Pb), as shown in Fig. 4(a). Thus, the first pulse and V(Ti) appear to have less impact on the incubation sequence than increasing V(Pb), which shortened the length of the incubation period.

Figure 5 shows the effective deposition rates of Pb and Ti as a function of V(Pb) calculated from the slopes in Fig. 4(b). It should be noted that the effective deposition rates given here have not been influenced by the incubation periods. As the Pb precursor input increases, the deposition rate of Pb increases accordingly, as does the deposition rate of Ti. It appears that the deposition rate of Ti is quite excessive under this high injection volume of Ti precursor compared to the Pb precursor injection. Therefore, for the lower V(Pb), the Pb deposition rate cannot match the deposition rate of Ti. With increasing V(Pb), the deposition rate of Pb becomes comparable to that of Ti, and the film becomes stoichiometric with respect to the cation ratio as shown in Fig. 6. With further increases in V(Pb), the Pb/Ti ratio becomes >1 as expected.

The incubation periods observed for the $8\times$(Ti–O)-1 $\times$(Pb–O) and $1\times$(Pb–O)-16$\times$(Ti–O) sequences were comparable as mentioned above. However, an obvious difference can be seen in the effective deposition rates of Pb and Ti. The deposition rates of Pb in the $8\times$(Ti–O)-1 $\times$(Pb–O) sequence with V(Pb) of 27 μl/cycle and in the $1\times$(Pb–O)-16$\times$(Ti–O) sequence with V(Pb) of 32 μl/cycle were 9×10^{-10} and 5×10^{-10} mol/cm^2 sequence, respectively. The differences between the two sequences are caused by the number of Ti–O cycles in one sequence and the precursor used for the first injection. Since the mole area density of Ti deposited in one sequence did not affect the deposition rate of Pb, as can be seen in Figs. 2(b) and 4(a), the order of the precursor injection is responsible for the higher deposition rate of Pb in the sequence that began with the first Ti precursor injection.

In contrast, the $8\times$(Ti–O)-1$\times$(Pb–O) and 1 $\times$(Pb–O)-16$\times$(Ti–O) sequences with V(Pb)$=$27 $\sim$32 μl/cycle had an identical deposition rate for Ti, 9×10^{-10} mol/cm^2 sequence, in spite of the large difference in the volume of Ti precursor supplied in one sequence (360 vs 617 μl/sequence). As can be seen in Fig. 4(a), increasing the input of the Ti precursor in one sequence led to a higher deposition rate when the order of precursor injection was the same. Therefore, this result suggests that the efficiency of the Ti precursor chemisorption is low in the sequence that began with the Pb precursor injection. Compared to the data given in Fig. 2(a) where the deposition rate of Ti saturates to $\sim1\times10^{-9}$ mol/cm^2 sequence for V(Pb)$>\sim$40 μl/cycle, the deposition rate of Ti continued to increase over this value with increasing V(Pb) up to a value of 161 μl/cycle. This is due to double the number of Ti–O cycles in one sequence and the higher overall injection volume of Ti precursor per cycle.

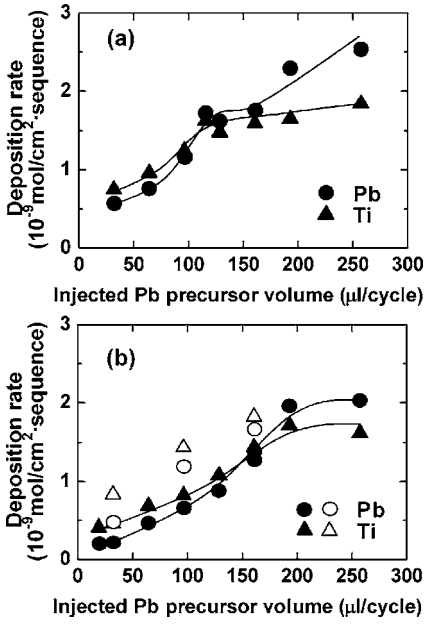

FIG. 7. Deposition rates of Pb and Ti as a function of the volume of injected Pb precursor. The volume of injected Ti precursor was fixed at 39 μl/cycle. Unit sequences of (a) 16×(Ti–O)-1×(Pb–O) (Ti starts) and (b) 1×(Pb–O)-16×(Ti–O) (Pb starts) were repeated 20 times. The open symbols in 7(b) indicate effective deposition rates displayed in Fig. 5.

Although both sequences with similar V(Pb) showed a comparable incubation period, the precursor, which was first supplied to the substrate, affected the effective growth rate after nucleation. We suppose that the first Ti precursor injection provided a higher nucleation density compared to the sequence with the first Pb precursor injection. The higher nucleation density will result in a higher growth rate and a higher efficiency of the precursors.

Here, two different growth sequences were adopted to test the chemisorption properties of the Pb and Ti precursors on the Pt surface: one is that the Ti precursor was injected first (Ti starts) and the other is that the Pb precursor was injected first (Pb starts). For all V(Pb) values, the Pb/Ti ratio showed a higher value for the Ti starts, as can be seen in Fig. 6.

Figures 7(a) and 7(b) show the variations in the Pb and Ti deposition rates as a function of V(Pb) in the Ti starts and Pb starts, respectively. This graph reveals several features of the ALD-$PbTiO_x$ process during the initial growth stage. First, the Pb and Ti deposition rates showed an initial increase with increasing V(Pb) and then saturated to a certain value for Ti, while Pb continued to increase, as shown in Fig. 7(a) (Ti start). Since 16 Ti–O cycles were repeated in one sequence, the saturated Ti growth rate was higher than that shown in Fig. 2. Second, when Pb starts was used, the overall deposition rate was retarded so that saturation of the growth rate occurred at a higher V(Pb). This saturation region probably corresponds to full coverage of the Ti–O surface. This result supports our hypothesis that the nucleation density may be enhanced by the first Ti precursor injection. Attention should be drawn to the fact that the deposition rates in Fig. 7 were obtained by dividing the measured area density by the number of total cycles including the incubation period. Open-symbol data points shown in Fig. 7(b) indicate the effective deposition rates, which were reproduced from the data shown in Fig. 5. The apparent deposition rates of Ti starts are still comparable to the effective deposition rates of Pb starts. Based on Fig. 4(a), a certain incubation period is expected for the Ti starts. Thus the effective deposition rate of Ti starts should be higher than the apparent deposition rate displayed in Fig. 7(a) and also higher than the effective deposition rate of Pb starts shown in Fig. 7(b). Although the effective deposition rates and incubation period were not systematically investigated for the Ti starts, the effective deposition rate in the Ti starts should be higher than those in the Pb starts.

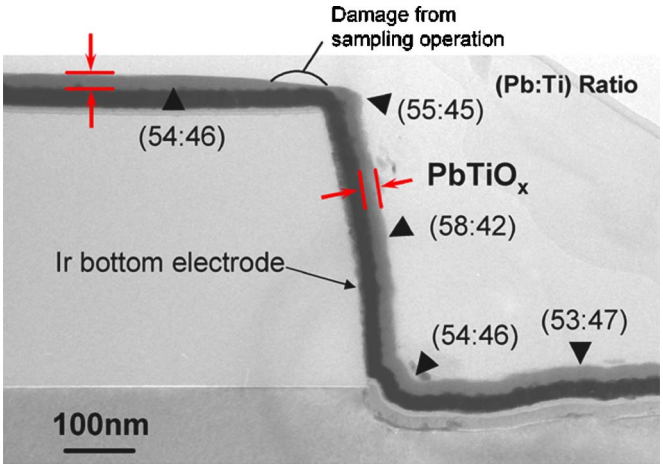

FIG. 8. (Color online) Cross sectional TEM image of a $PbTiO_x$ film deposited on a 3D substrate precoated with an Ir layer. Average Pb/Ti values attained from three to eight local EDS measurements are shown here.

C. Structural characterization of $PbTiO_x$ films

Figure 8 shows a cross sectional TEM picture of a $PbTiO_x$ film deposited on a substrate with hole structures of about 1.3 μm in diameter and 0.5 μm in depth precovered with an Ir bottom electrode layer. This $PbTiO_x$ film was deposited by repeating the Ti starts process 30 times with V(Pb) and V(Ti) of 129 and 39 μl/cycle, respectively. The $PbTiO_x$ film appeared to be amorphous. The film thickness was constant at about 15 nm over the whole structure. The local film composition was measured by EDX. The values displayed in Fig. 8 are average values of three to eight local measurements. The distribution of the Pb/Ti ratio over the hole structure was within ±10%. This distribution of cation composition is better than the large distribution of more than 30% reported for films deposited by MOCVD.[1,3,4] Although the process was not an ideally self-regulated one, the very slow gradient of the Pb/Ti ratio against V(Pb) shown in Fig. 6 could be the reason for better cation composition uniformity compared to MOCVD.

One $PbTiO_x$ film was annealed for crystallization. Figure 9 shows XRD patterns of a 15 nm thick $PbTiO_x$ film deposited on a planar substrate. Similar to TEM characterization, no peaks originating from the $PbTiO_3$ phase were detected for the as-deposited sample, even after annealing at 400 °C for 30 min in O_2 ambient, but peaks of 001/100 and/or 101/110 $PbTiO_3$ were observed after additional annealing at 500 or 600 °C for 10 min in O_2. Figure 10 shows the surface

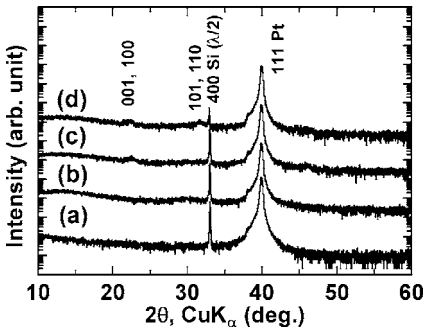

FIG. 9. XRD patterns of as-deposited and annealed $PbTiO_x$ films. (a) As-deposited $PbTiO_x$ film at 240 °C. (b) $PbTiO_x$ film annealed at 400 °C for 30 min in O_2 ambient. Subsequently, additional heat treatments were performed in O_2 ambient for the $PbTiO_x$ film which was already annealed at 400 °C. $PbTiO_x$ film after second annealing at (c) 500 °C for 10 min and (d) 600 °C for 10 min.

morphology in a 5×5 μm^2 array of the as-deposited and annealed $PbTiO_x$ films ($t=15$ nm) as observed by AFM. The as-deposited $PbTiO_x$ film, which is considered to be amorphous, showed no particular grain structure, while a significant granular structure was confirmed for the annealed $PbTiO_x$ films. The values of the root mean square surface roughness (R_{rms}) of the $PbTiO_x$ films were 1.8 nm (as-deposited), 2.2 nm (400 °C for 30 min and 500 °C for 10 min), and 2.3 nm (400 °C for 30 min and 600 °C for 10 min). The R_{rms} of the Pt-covered Si substrate was 0.9 nm. The residual C content in the $PbTiO_x$ films prepared at 240 °C was characterized by XPS after 1 min sputtering to remove surface adsorbates. The $PbTiO_x$ films contained only 2 at. % of C in spite of the low deposition temperature and liquid source injection with solvent.

IV. CONCLUSIONS

$PbTiO_x$ films were deposited at 240 °C on Pt-covered Si substrates by liquid injection ALD using $Ti(Oi\text{-}Pr)_2(DPM)_2$ and $Pb(DPM)_2$ dissolved in ethylcyclohexane. In the $PbTiO_x$ process, the deposition rates of Pb and Ti were dramatically enhanced compared to their binary ALD processes. The high deposition rate of Ti in the $PbTiO_x$ process was ascribed to a high bonding site density on the Pb–O layer or to an active chemisorption reaction with the Pb–O layer. Due to this strong interaction, the number of bonding sites provided by the underlying Pb–O layer defined the deposition rate of Ti, so that the Pb/Ti ratio and the deposition rates of Pb and Ti were self-regulated for excess Ti precursor supply.

The deposition rate of Pb increased with an increasing input of Pb precursor until full coverage was achieved, and then showed a narrow window where the deposition rates of both Pb and Ti were constant. For further Pb precursor injection, the deposition rate of Pb again increased probably because of catalytic decomposition of the Pb precursor by the Ti–O layer. As a result, a clear plateau region was not observed for the Pb/Ti ratio as a function of the volume of injected Pb precursor. The original ALD-PbO and TiO_x processes showed a self-limiting growth rate. However, the combination process for $PbTiO_x$ film growth was not a self-regulated one. It was therefore concluded that the interface chemistry between the precursors and the predeposited cation layer has a critical impact on the self-regulated growth mode in the multicomponent oxide ALD process.

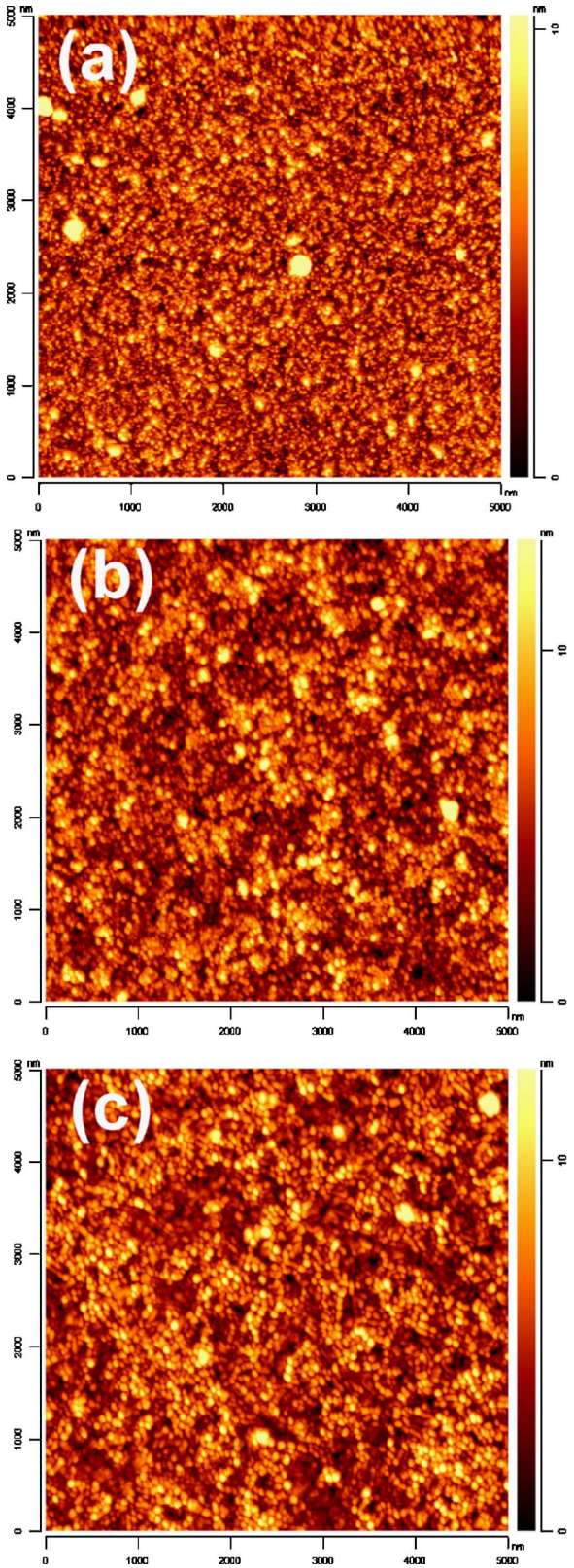

FIG. 10. (Color online) Surface morphologies of (a) as-deposited $PbTiO_x$ film ($t=15$ nm) at 240 °C and annealed $PbTiO_x$ films in O_2 under conditions of (b) 400 °C for 30 min+500 °C for 10 min and (c) 400 °C for 30 min+600 °C for 10 min. XRD patterns of these films are shown in Figs. 9(a), 9(c), and 9(d), respectively.

There was a common incubation period for the growth of Ti–O and Pb–O layers. This incubation period was not significantly affected by the input of the Ti precursor and the order of the precursor injection, while it was clearly shortened by increasing the input of the Pb precursor. We would like to emphasize that this variable incubation sequence is a potential key issue when addressing the uniform coverage of 3D structures. A sequence that began with Ti precursor injection showed higher deposition rates for both Pb and Ti compared to a sequence starting with Pb precursor injection. We supposed that the first Ti precursor injection contributed to the generation of a high-density bonding site for the chemisorption process so that the growth rate and efficiency of the precursors were enhanced.

Although the present $PbTiO_x$ process did not have an ideal process window in the cation composition, the resulting $PbTiO_x$ film deposited on a 3D substrate exhibited uniform step coverage and better uniformity of cation composition compared to MOCVD films. We believe that the present uniformity in cation composition can be improved by optimizing the interface chemistry.

ACKNOWLEDGMENTS

The authors would like to thank Dr. A. Besmehn for XPS analysis, W. Krumpen for XRF analysis, M. Gebauer and M. Gerst for their technical support, and L. Cattaneo, S. Carella (SAES Getters S.p.A), and Dr. Y. Tasaki (Toshima MFG Co., Ltd.) for fruitful discussions. SAES Getters S.p.A is gratefully acknowledged for supplying the precursors. The 3D substrates were kindly provided by Samsung Advanced Institute of Technology (SAIT). One of the authors (T.W.) would also like to extend thanks to the Alexander von Humboldt Stiftung (AvH) for awarding him a research fellowship. Another author (C.S.H.) also acknowledges the support of AvH for this collaboration.

[1] A. Nagai, J. Minamidate, G. Asano, C. J. Choi, C.-R. Cho, Y. Park, and H. Funakubo, Electrochem. Solid-State Lett. **9**, C15 (2006).
[2] A. Nagai, G. Asano, J. Minamidate, C. J. Choi, C.-R. Cho, Y. Park, and H. Funakubo, Mater. Res. Soc. Symp. Proc. **830**, D2.2 (2005).
[3] C. S. Hwang, J. Park, D. S. Hwang, and C. Y. Yoo, J. Electrochem. Soc. **148**, G636 (2001).
[4] C. S. Hwang, S. Y. No, J. Park, H. J. Kim, H. J. Cho, Y. K. Han, and K. Y. Oh, J. Electrochem. Soc. **149**, G585 (2002).
[5] L. Niinistö, J. Päiväsaari, J. Niinistö, M. Putkonen, and M. Nieminen, Phys. Status Solidi A **201**, 1443 (2004).
[6] H. Kim, J. Vac. Sci. Technol. B **21**, 2231 (2003).
[7] R. L. Puurunena, J. Appl. Phys. **97**, 121301 (2005).
[8] S. Y. Chou, P. R. Krauss, and P. J. Renstrom, J. Vac. Sci. Technol. B **14**, 4129 (1996).
[9] S. R. Summerfelt *et al.*, Appl. Phys. Lett. **79**, 4004 (2001).
[10] S. R. Gilbert *et al.*, J. Appl. Phys. **93**, 1713 (2003).
[11] T. Watanabe, S. Hoffmann-Eifert, C. S. Hwang, and R. Waser, Mater. Res. Soc. Symp. Proc. **902E**, 0902-T04–07.1 (2006).
[12] T. Watanabe, S. Hoffmann-Eifert, C. S. Hwang, and R. Waser, J. Electrochem. Soc. **153**, F199 (2006).
[13] H. Seim, H. Mölsä, M. Nieminen, H. Fjellvåg, and L. Niinistö, J. Mater. Chem. **7**, 449 (1997).
[14] M. Vehkamäki, T. Hänninen, M. Ritala, M. Leskelä, T. Sajavaara, E. Rauhala, and J. Keinonen, Chem. Vap. Deposition **4**, 227 (1998).
[15] M. Vehkamäki, T. Hatanpää, T. Häanninen, M. Ritala, and M. Leskelä, Electrochem. Solid-State Lett. **2**, 504 (1999).
[16] M. Schuisky, K. Kukli, M. Ritala, A. Hårsta, and M. Leskelä, Chem. Vap. Deposition **6**, 139 (2000).
[17] M. Nieminen, T. Sajavaara, E. Rauhala, M. Putkonen, and L. Niinistö, J. Mater. Chem. **11**, 2340 (2001).
[18] M. Nieminen, S. Lehto, and L. Niinistö, J. Mater. Chem. **11**, 3148 (2001).
[19] W. C. Shin *et al.*, Electrochem. Solid-State Lett. **7**, F31 (2004).
[20] O. S. Kwon, S. K. Kim, M. Cho, C. S. Hwang, and J. Jeong, J. Electrochem. Soc. **152**, C229 (2005).
[21] J. Harjuoja, A. Kosola, M. Putkonen, and L. Niinistö, Thin Solid Films **496**, 346 (2006).
[22] Y. Otani, S. Okamura, and T. Shiosaki, Jpn. J. Appl. Phys., Part 1 **45**, 1752 (2006).
[23] J. S. Zhao, J. S. Sim, H. J. Lee, D.-Y. Park, and C. S. Hwang, J. Electrochem. Soc. **153**, F81 (2006).
[24] W. D. Kim *et al.*, J. Electrochem. Soc. **152**, C552 (2005).
[25] S. K. Kim and C. S. Hwang, J. Appl. Phys. **96**, 2323 (2004).
[26] A. Furuya, K. Yoneda, E. Soda, T. Yoshie, H. Okamura, M. Shimada, N. Ohtsuka, and S. Ogawa, J. Vac. Sci. Technol. B **23**, 2522 (2005).